Mode Dependence of Vibrational Energy Redistribution in Nickel Tetraphenylporphyrin Probed by Picosecond Time-Resolved Resonance Raman Spectroscopy: Slow IVR to Phenyl Peripherals

Yasuhisa Mizutani# **and Teizo Kitagawa***,†

Institute for Molecular Science, Okazaki National Research Institutes, Myodaiji, Okazaki 444-8585

†Center for Integrative Bioscience, Okazaki National Research Institutes, Myodaiji, Okazaki 444-8585

(Received September 7, 2001)

The formation of the (d, d) excited state of (*meso*-tetraphenylporphyrinato)nickel(II) ([Ni(tpp)]) upon (π, π^*) excitation, and its vibrational energy relaxation were monitored by picosecond time-resolved resonance Raman spectroscopy. Stokes resonance Raman bands due the (d, d) excited state instantaneously appeared upon the photoexcitation into the (π, π^*) excited state. Their intensities decayed with a time constant of about 250 ps, which corresponds to electronic relaxation from the (d, d) excited state to the electronic ground state. This is consistent with the results of ultrafast absorption measurements reported by Eom et al. [H. S. Eom, S. C. Jeoung, D. Kim, J. H. Ha, and Y. R. Kim, *J. Phys. Chem. A*, **101**, 3661 (1997)]. Anti-Stokes ν_4 (macrocycle in-plane mode) intensities of [Ni(tpp)] in the (d, d) excited state appeared promptly and decayed with a time constant of 3.6 ± 0.6 ps. The rise and decay of anti-Stokes intensity are interpreted as vibrational excitation due to the excess energy and intermolecular vibrational energy transfer to the surrounding solvent molecules, respectively. The ϕ_4 mode, which is mainly ν(CC) of the peripheral phenyl groups, gave no detectable anti-Stokes intensity although the mode gave appreciable Stokes intensity. This means that the ϕ_4 mode is left vibrationally less excited than the ν_4 mode in the process of vibrational energy relaxation and that intramolecular vibrational energy redistribution is not completed in a subpicosecond time regime. These results for [Ni(tpp)] demonstrate that the vibrational modes of peripheral groups are vibrationally less excited shortly after the formation of the (d, d) excited state and that energy redistribution in the peripheral groups takes place in picoseconds, such a short time is competitive with vibrational energy transfer to the surrounding solvent molecules.

Vibrational energy relaxation (VER) plays an essential role in many chemical processes in condensed phases and hence has attracted much attention.[1–3] Upon photoexcitation, some excess energy is initially deposited in Franck–Condon active vibrations. Right after nonradiative transition, the energy is localized in some specific vibrational modes.[4–6] Subsequent thermal equilibration processes are not fully understood for the excited molecules in solutions. In a picture for a polyatomic molecule in gas phase, the energy relaxation process would be composed of two temporally distinct steps: intramolecular vibrational energy redistribution (IVR) among all vibrational freedoms of the molecule and intermolecular energy transfer (IET) to other molecules by collisions and other means. For large molecules in solution, the time scales of IVR and IET are not clear due to lack of detailed studies. IET is found to occur on the time scale of 1 – 100 ps, while IVR is generally believed to occur on the subpicosecond time scale for large molecules in solution,[1,3] although there has been no clear experimental evidence for this. Standard theoretical descriptions of solution phase reactions such as RRKM theory employ the reaction coordinate picture in which modes orthogonal to the reactive motion are considered to remain in statistical distribution with one another and also with modes of the solvent during the course of the reaction. While this may be a good approximation on the time scale of activated processes in which IVR is faster compared with barrier crossing, it is not expected to hold in the reactions with low or no barrier. In such cases, the motion along the reaction coordinate can occur on time scales comparable to, or even slower than IVR, and therefore, statistical description of the reaction is no longer appropriate. Microscopic understanding of solvent-induced vibrational relaxation processes is essential to provide a detailed picture of chemical reactions.

Vibrational relaxation dynamics in the condensed phase has been extensively studied with time-resolved pump–probe optical spectroscopy.[7–10] The thermally enhanced, low frequency tail of the absorption spectrum (or the high energy part of the emission spectrum) arising from vibrationally excited states gives information on the transient temperature of the vibrational system. However, the interesting questions concerning the initial energy distribution and the detailed pathway to a thermal distribution are not easily answered by this kind of experiments, since usually the vibronic structures of the electronic transition are not spectrally resolved for solutions. On the other hand, time-resolved Raman and infrared techniques allow, at least in principle, more direct monitoring of vibrational populations because their energy resolution is much higher than

---

Present address: Molecular Photoscience Research Center, Kobe University, Nada, Kobe 657-8501

visible absorption or emission spectroscopy. Especially, time-resolved anti-Stokes Raman spectroscopy is selective for vibrationally excited modes and therefore is powerful to measure VER.[11–14] The ratio of the integrated areas of anti-Stokes to Stokes scattering, corrected to the first order for reabsorption and cross section differences, is expected to provide the most direct information about relative vibrational populations,[15,16] and is therefore essential to studies of energy distribution dynamics in molecular systems. Recently picosecond time-resolved resonance Raman (TR^3) studies on the time scale of IVR have been reported.[12–14,17–22] Some of them claimed the assumption that IVR is much faster than IET for large molecules in solution.[12–14,18,19,21,22]

We have been studying the VER of nickel porphyrins in solution. Nickel porphyrins are chosen as the subject of study for several reasons. First, molecular vibrations of nickel porphyrins in the electronic ground state have been well characterized through resonance Raman and IR experiments and normal coordinate analysis.[23–27] Second, an electronically excited nickel porphyrin reaches the (d, d) excited state in a very short time (<350 fs),[28] transferring most of the electronic energy into the vibrational degrees of freedom. Nickel porphyrins have absorption bands in the visible and near UV regions due to (π, π^*) transition of porphyrin ring. The photochemistry of nickel porphyrins has been studied by transient absorption spectroscopy;[28,29] results have shown that photoexcitation of nickel porphyrins in noncoordinating solvents, such as toluene and benzene, leads to the formation of a relatively long-lived metal excited state, B_{1g}, via nonradiative transition from the (π, π^*) state. This nonradiative transition deposits an excess energy of ~10,000 cm^{-1} into the vibrational manifold of the macrocycle. The decay of the (d, d) excited state into the A_{1g} ground state takes place in about 300 ps. Therefore, there is reasonable separation on time scale between the expected vibrational relaxation and the electronic relaxation. Finally, the S_0–S_1 (Q band) and S_0–S_2 (B band) absorption bands are reasonably separated and thus suitable to use them for effective population of excited state and resonance enhancement of Raman intensity in pump-probe Raman experiments.

We have previously demonstrated that the statistical energy distribution has not been achieved in a picosecond time scale for (octaethylporphyrinato)nickel(II) ([Ni(oep)]) in benzene using TR^3 spectroscopy.[13] The rise of anti-Stokes intensities of [Ni(oep)] upon the photoexcitation was not uniform: the rise of the ν_4 anti-Stokes intensity was instantaneous, while the rise of the ν_7 anti-Stokes intensity was delayed by 2.6 ± 0.5 ps. This delay indicates that there is a non-Boltzmann distribution in vibrational manifold in the initial few picoseconds.

The present paper reports the VER of (*meso*-tetraphenylporphyrinato)nickel(II) ([Ni(tpp)]), which is another representative type of porphyrins. It is the aim of the present study to clarify the time evolution of excited vibrational populations in an electronically excited molecule by measuring changes of Stokes and anti-Stokes intensities of [Ni(tpp)], especially, focusing on intensity of anti-Stokes bands of phenyl peripheral modes. We discuss vibrational energy redistribution in phenyl peripherals of [Ni(tpp)] and demonstrate that vibrational energy redistribution into the phenyl peripherals of [Ni(tpp)] is slow compared to energy dissipation into the solvent molecules.

Experimental

Laser System. The details of the TR^3 apparatus used in this study are described elsewhere.[30] Briefly, a picosecond mode-locked Ti:sapphire oscillator (Spectra-Physics, Tsunami 3950), pumped by an Ar^+ ion laser (Spectra-Physics, BeamLok 2060), produced about 1.5-ps wide pulses. The seed pulse was amplified by a regenerative amplifier (Positive Light, Spitfire) operated at 1 kHz. This amplification unit provides 770-nm pulses, each with an energy of about 0.8 mJ and duration of 2.5 ps. In the pump arm, a pump pulse of 532 nm was generated with a home-built optical parametric generator (OPG) and amplifier (OPA). The 532-nm pulses were used for the pump beam for the ps-TR^3 measurements after they were attenuated to 10 μJ. In the probe arm, a probe pulse of 458 nm was generated as the first Stokes stimulated Raman scattering from compressed hydrogen gas (50 kg/cm^2) excited by the second harmonic of the 770-nm output. Components other than the first Stokes scattering were removed spectrally with a glass filter and dichroic mirrors and spatially with a Pellin-Broca prism. The energy and bandwidth of the generated 458-nm pulses were about 1.0 – 1.5 μJ and about 15 cm^{-1}, respectively. The 458-nm pulses were used for the probe beam after they were attenuated to 0.1 μJ. The pump and probe beams were made collinear and coaxial using a dichroic mirror. The polarization of the pump beam was rotated by 55° relative to that of the probe beam to minimize the effects of molecular rotations on the observed kinetics. Pulse energies of the two beams were always monitored with photodiodes (Hamamatsu Photonics, S2387-1010R) and were found to be stable within ±10%. A cross correlation trace of the pump and probe pulses was measured with a 1-mm BBO crystal, which indicated a width of 2.3 ps. The 0.0 ps of delay time (uncertainty < 0.2 ps) was calibrated using the sum frequency generation by the same crystal.

Data Acquisition. The sample solution was contained in a 10-mmϕ NMR tube and spun with a spinning cell device. The sample was spun at 3400 rpm in the spinning cell configured for 135° backscattering illumination and collection to minimize the effects of molecular rotations on the observed kinetics.[31] Spherical and cylindrical lenses were used to focus the pump and probe beams on the sample in line-focusing condition. The laser flux of the pump and probe pulses was ~500 and ~7 MW/cm^2, respectively. About 8% of the initially present ground state molecules were pumped to form a sufficient number of vibrationally excited (d, d) state molecules to be observed. This does lend further support to the conclusion that the ground state population is not seriously depleted under the present experimental conditions.

Raman scattering was collected and were imaged onto the 200-μm entrance slit of a single spectrometer (Spex, 500M). A holographic notch filter (Kaiser Optical Systems, HSNF-457.9-1.0) was used to reject the unshifted scattering. The dispersed light was detected by a liquid-nitrogen-cooled CCD detector (Princeton Instruments, CCD-1100PB). Raman shifts were calibrated with cyclohexane, benzene, or carbon tetrachloride. The peak positions of Raman bands are accurate within ±2 cm^{-1}.

Sample Preparation. [Ni(tpp)] and [Fe(tpp)(Cl)] (Aldrich Chemical Co.) were used without further purification. Benzene was of spectroscopic grade (Dojindo Laboratories). Solutions with the [Ni(tpp)] concentrations from 0.03 mM to 0.3 mM were examined and no concentration dependence of kinetics was observed. Sample integrity was confirmed with UV-visible absorption spectra after the TR^3 measurements.

Results and Discussion

Stokes Spectra. Figure 1 shows Stokes-TR^3 spectra of the [Ni(tpp)] photoproduct in benzene. The delay times of the probe pulse from the pump pulse are indicated at the left side of each spectrum. In these spectra, the contribution of unreacted species has been subtracted and signal intensities are corrected using the intensity of solvent band at 992 cm^{-1} to eliminate the effect of self-absorption of the sample. The probe-without-photolysis spectrum (ground state spectrum) is given at the bottom of the figure for comparison. This spectrum is in agreement with the reported spectrum.[25]

In negative delay times, the difference spectra are absolutely featureless. In positive delay times new bands appeared; these indicate the generation of a photoproduct. Their intensities increased up to 4 ps, and then gradually decreased with time. Their peak positions gradually shifted upward until 20 ps being accompanied by band narrowing, and no further evolution was observed after 20 ps. Similar peak shifts and band narrowing were also observed in the TR^3 spectra of [Ni(oep)] that were reported previously and were ascribed to VER in the (d, d) excited state.[13] The difference spectrum was absolutely featureless at 1 ns of delay time, indicating that the photoproduct has completely returned into the ground-state species. The bands in the 100-ps delay spectrum at 1078, 1232, 1359, 1553, and 1599 cm^{-1} are assigned to ν_9, ν_1, ν_4, ν_2 and ϕ_4 modes, respectively, on the basis of the ground state spectra.[25] The observed Raman spectrum for the ground state species is consistent with that reported previously. There is no evidence for appearance of an additional electronic excited state in the TR^3 spectra.

The ν_1, ν_4, and ν_2 bands for the (d, d) excited state showed appreciable downshifts compared with those for the electronic ground state. These modes are totally symmetric in-plane modes; $\nu(C_mPh)$ (ν_1), $\nu(\text{Pyr half-ring})_{\text{sym}}$ (ν_4), and $\nu(C_\beta C_\beta)$ (ν_2). The low frequency shifts can be ascribed to the change in the core size of the [Ni(tpp)] macrocycle in the (d, d) excited state. In the (d, d) excited state in non-coordinating solvents, one d electron is promoted from the d_{z^2} orbital into the $d_{x^2-y^2}$ orbital. The promotion of the d electron would increase the effective size of the metal atom. This is because the $d_{x^2-y^2}$ orbital points at the pyrrole nitrogens of the porphyrin macrocycle. All the skeletal mode frequencies above 1450 cm^{-1} show a negative linear dependence on the core size, d[33–36], defined as the distance between the center of the porphyrin ring and the pyrrole nitrogen atoms, when this relationship is examined for metal complexes of tpp,[37] oep,[36] and protoporphyrin[35,37]; $\nu = K(A - d)$, where K and A are parameters characteristic of the porphyrin macrocycles. Employing the reported values of parameter K for the ν_2 mode of tpp's (297 cm^{-1}/Å),[38] one can evaluate the expansion (Δd) of the core sizes in the (d, d) excited state from that in the ground state of [Ni(tpp)] as $+0.064 \pm 0.008$ Å, which is slightly larger than that observed for [Ni(oep)].[13] Thus, the core size in the (d, d) excited state is calculated to increase to 2.02 Å from 1.96 Å[39] of the electronic ground state. The value (2.02 Å) of expanded core size in the (d, d) excited state is close to that of [Fe(tpp)(Cl)] (high spin) in the electronic ground state.[40] On the other hand, observed downshifts of the ν_9 and ϕ_4 bands upon the (d, d) excitation are very small. This is reasonable, because both modes are expected to be insensitive to the change in the core size of [Ni(tpp)]: the ν_9 mode contains mainly $\delta(C_\beta H)$ character and the ϕ_4 mode is mainly due to $\nu(CC)$ of the phenyl group.[25]

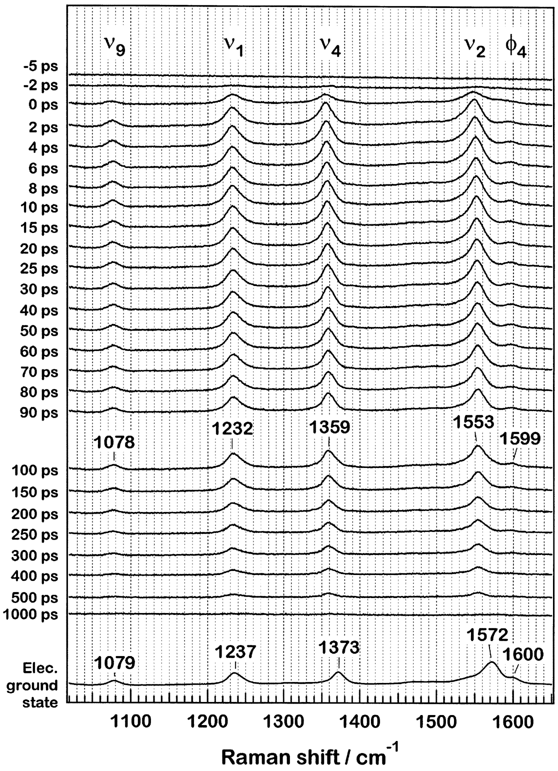

Fig. 1. Stokes TR^3 spectra of photoproduct of [Ni(tpp)] in benzene. The pump–probe delay times are indicated at the left side of each spectrum. In these spectra the contribution from unreacted species has been subtracted and signal intensities are corrected using the intensities of solvent bands (992 cm^{-1}) to eliminate the effect of self-absorption of the sample. The probe-without-photolysis spectrum is given at the bottom of the figure for comparison.

Stokes RR intensities provide us information on the electronic population of the molecule because they are proportional to the population if the intensities are corrected for the effect of self absorption. To see the intensity change quantitatively, the Stokes ν_4 (squares) and ν_1 (triangles) band intensities are plotted against the delay time in Fig. 2. In the curve fitting calculations, the system response was deconvoluted from the Stokes intensity change using a Gaussian fit (the corresponding cross correlation width is 2.3 ps) to the cross-correlation signal. These temporal changes are well described with a single exponential decay with a time constant of 245 ± 10 and 269 ± 25 ps for ν_4 and ν_1 bands, respectively, as are delineated with solid curves in Fig. 2. These numbers are close to the lifetime of the (d, d) excited state reported by Eom et al.[29] The rising parts for the bands indicate that both bands appeared promptly within the instrument response time, consistent with the fact that nonradiative transition from the (π, π^*) excited state to the (d, d) excited state occurs within 350 fs.

Anti-Stokes Spectra. Anti-Stokes scattering reflects the excited state populations of individual vibrational modes. Fig-

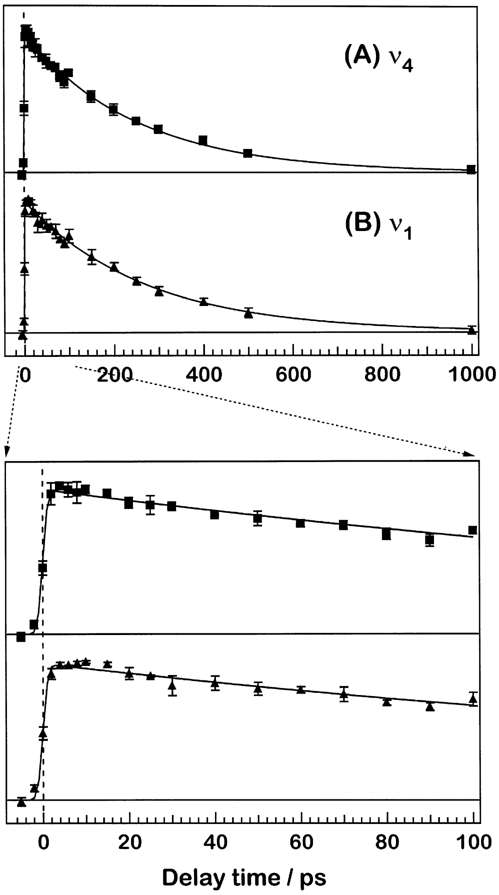

Fig. 2. Temporal change of Raman intensities of the Stokes ν_4 (squares) and ν_1 bands (triangles) of [Ni(tpp)] in the (d, d) excited state. The curves are displaced for clarity. The horizontal lines correspond to zero Raman intensity for each Raman band. The solid lines are calculated for instantaneous rise followed by a single exponential decay convoluted with a Gaussian instrument response function for which the cross correlation time is 2.3 ps. The best fit was obtained by decay time constants of 245 ± 15 and 269 ± 25 ps for ν_4 and ν_1 bands, respectively. The lower panel shows a closeup of the curve in the early time region.

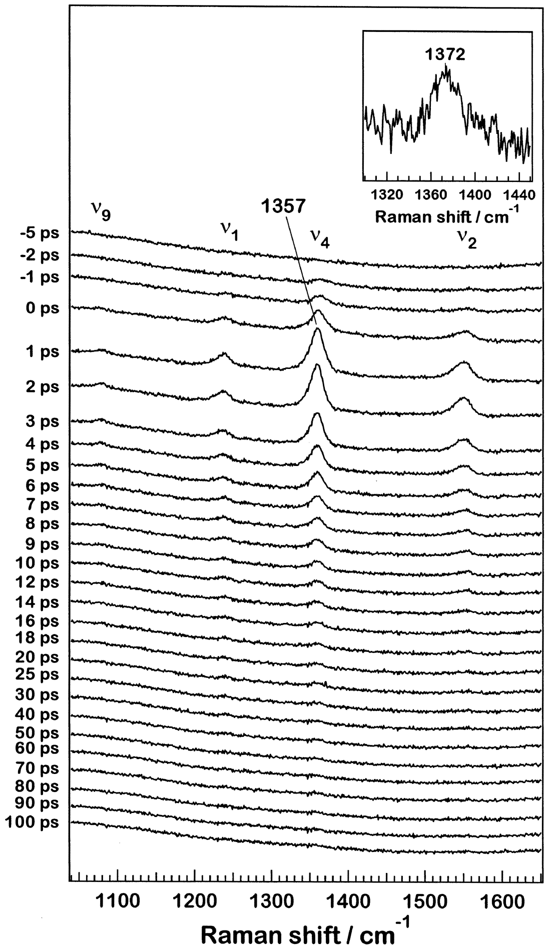

Fig. 3. Anti-Stokes TR^3 spectra of the photoproduct of [Ni(tpp)] in benzene. The pump-probe delay times are specified at the left side of each spectrum. In these spectra signal intensities are corrected using the intensities of solvent band (992 cm^{-1}) to eliminate the effect of self-absorption of the sample. The inset shows the probe-without-photolysis spectrum. Note that there is no anti-Stokes intensity at the position of ν_4 band of the (d, d) excited state.

ure 3 shows anti-Stokes TR^3 spectra of the photoproduct of [Ni(tpp)] in benzene. The anti-Stokes ν_1, ν_4 and ν_2 bands are most prominent, but ν_9 band is weakly seen. In these spectra, the contribution of unreacted species has been subtracted. As shown in the inset, the ν_4 band in the spectrum without photolysis gave the contribution from the electronic ground state and there is no intensity at the frequency of the (d, d) excited state. This indicates that the probe pulse is weak enough to prevent multiple interactions (i.e. absorption and Raman scattering) by a single porphyrin molecule over the duration of the probe pulse. With high photon flux, the ν_4 band of both electronic ground and the (d, d) excited states appeared, indicating that there is a significant probability for [Ni(tpp)] to be photoexcited and to provide Raman scattering within a single probe pulse under high photon flux. The absence of band intensity of the (d, d) excited state in the spectrum without photolysis is a good measure of adoption of a proper experimental condition for the probe power. In Fig. 3, new bands appear upon photoexcitation by the pump pulse, similar to Stokes spectra, but their intensity decays are faster than those of Stokes bands.

Figure 4 shows the temporal change of the Raman intensity of the anti-Stokes ν_1, ν_4 and ν_2 bands of [Ni(tpp)]. The temporal behaviors of these bands can be described with a single exponential function as delineated with solid lines. The best fit to the data by a single exponential yielded the decay constants of 3.5 ± 0.9, 3.6 ± 0.6 and 3.7 ± 0.6 ps for the ν_1, ν_4 and ν_2 bands, respectively. The decay should be ascribed to vibrational energy relaxation, because there is no such component in Stokes spectra. Note that the C$_m$–Ph stretching (ν_1) is vibrationally excited similar to the in-plane vibrations of the macrocycle. Since these anti-Stokes intensities decay in nearly the same way, it is suggested the excess energy is released to the surrounding solvent molecules in this time scale. Concerning the intensity rise, these anti-Stokes bands show the instrument-limited rise, same as the Stokes counterpart.

An interesting aspect is how much the excess energy is deposited into the peripheral modes of [Ni(tpp)]. Figure 5 com-

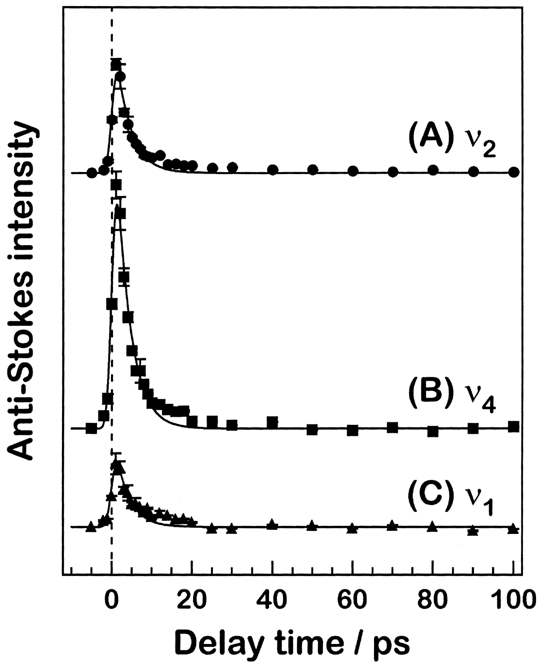

Fig. 4. Temporal change of the Raman intensity of the anti-Stokes ν_2 (A), ν_4 (B), and ν_1 (C) bands of [Ni(tpp)] in the (d, d) excited state. The best fit was obtained by decay time constants of 3.7 ± 0.6, 3.6 ± 0.6, and 3.5 ± 0.9 ps for ν_2, ν_4, and ν_1 bands, respectively.

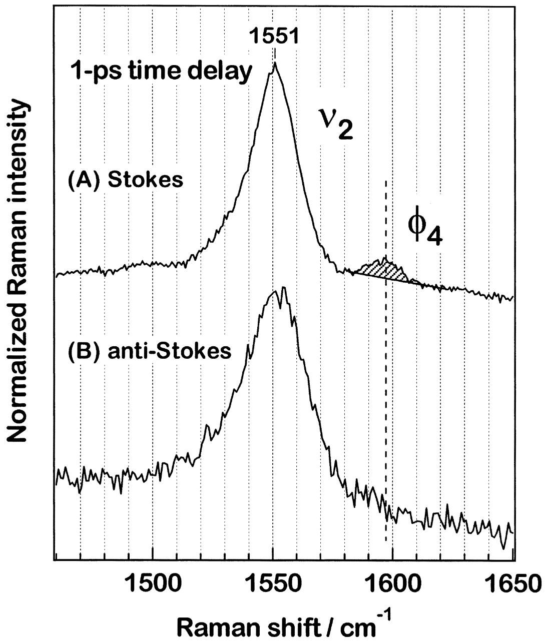

Fig. 5. Comparison of time-resolved Stokes and anti-Stokes spectra at 1-ps time delay.

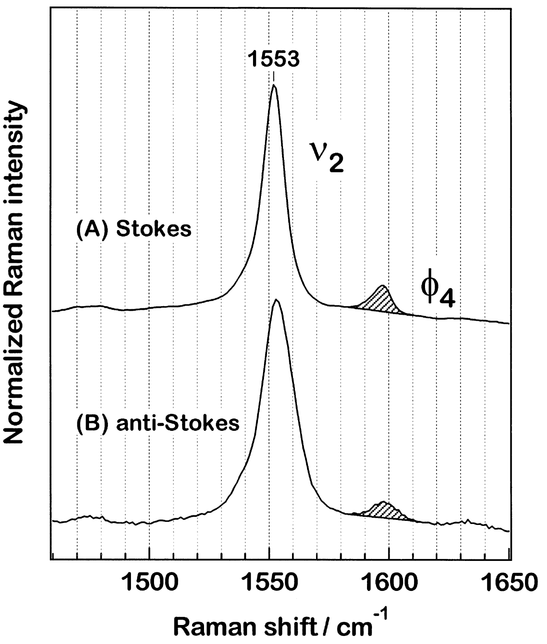

Fig. 6. Comparison of Stokes and anti-Stokes spectra of [Fe(tpp)(Cl)] in benzene. The spectra were measured with the 457.9-nm line from a CW Ar^+ ion laser.

pares time-resolved Stokes and anti-Stokes spectra at 1-ps time delay. The ϕ_4 mode is present at 1599 cm^{-1} in the Stokes spectrum, but in contrast, the band is absent in the anti-Stokes spectrum. We have two possible reasons for very weak anti-Stokes ϕ_4 intensity. One is less population at vibrationally excited levels of the ϕ_4 mode. Another idea is that this is due to small resonance Raman cross section of anti-Stokes scattering of this mode, because, in the case of resonance condition, Raman cross section of anti-Stokes scattering is not same as that of Stokes scattering.

In order to examine the latter possibility, we measured resonance Raman spectra of [Fe(tpp)(Cl)] in benzene at room temperature using a CW laser of the same probe wavelength as that used for TR^3 measurements of [Ni(tpp)]. The results are shown in Fig. 6. [Fe(tpp)(Cl)] in the electronic ground state (high spin) has a comparable core size (2.02 Å) to that of [Ni(tpp)] in the (d, d) excited state as noted above.[40] Therefore it is expected to give an RR spectrum similar to that of [Ni(tpp)] in the (d, d) excited state. In fact these two species give very similar spectra. Because the RR spectra were measured with a CW laser, observed anti-Stokes intensities reflect statistical distribution of vibrational populations at room temperature. In statistical distribution, ϕ_4 mode has a detectable intensity even at room temperature as shown here. This result shows that the intensity difference in [Ni(tpp)] is not due to the difference in Raman cross section between the Stokes and anti-Stokes scattering, and hence must be attributed to lower population of vibrationally excited levels of ϕ_4 mode. In the course of the relaxation, the anti-Stokes ϕ_4 band was not observed at any time delay for [Ni(tpp)]. This implies that the ϕ_4 mode is vibrationally less excited than the in-plane vibrational modes on the formation of the (d, d) excited state, and is left less excited in the process of relaxation, indicating that vibrational energy redistribution into the phenyl peripherals of [Ni(tpp)] is slower than energy dissipation into the solvent molecules. This fact is unexpected, because the recognizable anti-Stokes intensity of the ν_1 (mainly C_m–Ph stretching) mode suggested that the excess energy has reached to the C_m–Ph bond as noted before.

The present results cannot be explained by the idea that energy randomization within the molecule occurs on the subpicosecond timescale, which is generally believed to occur for large molecules.[1,3] For large molecules with dense vibrational manifolds, the following scheme of the relaxation process involving two temporally distinct steps has been proposed.[1,3,7,8,41–43]

$$A \xrightarrow{\text{IVR}} B \xrightarrow{\text{IET}} C$$

Here A represents the state initially prepared by optical excitation or nonradiative transition with a non-statistical distribution of vibrational energy, B is a state characterized by a Boltzmann distribution of high vibrational energy,[44] and C is a thermally equilibrated state at ambient temperature. The validity of this picture relies on a clear separation in time scales between the intra- and intermolecular energy transfer processes. Experimental data which support this picture have been obtained by ultrafast transient absorption and emission studies.

In the absence of such a separation, the loss of energy to the solvent competes with the internal redistribution process; as a result, the solute may never achieve a Boltzmann distribution of the excess energy. In fact, several recent experiments have suggested that the IVR is not completed within a few picoseconds for large molecules in solutions, such as stilbene,[9,12,19] bacteriorhodopsin,[45] metalloporphyrins,[13,46–48] 2-(2′-hydroxy-5′-methylphenyl)benzotriazole,[49] and betaine-30.[14] We have previously demonstrated that the statistical energy distribution has not been achieved on a picosecond time scale for [Ni(oep)] in benzene using TR^3 spectroscopy.[13] The rise of the ν_4 anti-Stokes intensity was instantaneous, while the rise of the ν_7 anti-Stokes intensity was not instantaneous but was delayed by 2.6 ± 0.5 ps. This delay indicated that there is a non-Boltzmann distribution in vibrational manifold in the initial few picoseconds. The present study shows that the statistical energy distribution between the skeletal and peripheral modes has not been achieved in a picosecond time scale for [Ni(tpp)].

The phenyl groups of tpp are prevented from rotating into coplanar orientation with respect to the porphyrin ring by steric repulsion between the phenyl ortho H atoms and the pyrrole C_β H atoms.[50] Consequently conjugation is expected to be unimportant in the tpp ground state. Consistent with this view, NMR data show the relatively small contact shifts of the phenyl protons in low-spin iron(III) complexes of *meso*-substituted porphyrins.[51] It has been suggested that the RR enhancements seen for the phenyl modes reflect delocalization in the excited state.[52] The vibrational character of the ϕ_4 mode was calculated to be composed of $\nu(\text{CC})_{\text{ph}}$ (61%), $\delta(\text{CCH})$ (20%), and $\nu(\text{C}_\text{m}\text{C}_{\text{ph}})$ (13%).[25] The vibrational motion of the ϕ_4 mode would not involve the motion of atoms of π-conjugated system. This suggests weak anharmonic coupling of the ϕ_4 mode to the skeletal modes, which leads to inefficient exchange of vibrational energy between them. On the contrary, vibrational mixing between the ϕ_4 mode and the skeletal modes was suggested in the normal mode analysis of [Ni(tpp)].[25] The present results favor the idea that the vibrational mixing is not so significant. One may argue that the electronic delocalization could lead to the vibrational excitation of the ϕ_4 mode on the photoexcitation to the (π, π*) excited state. In the present experimental condition, however, the 532-nm pump pulse does not give a large excess energy to [Ni(tpp)] on the photoexcitation, because the energy of the 532-nm photon is close to the 0–0 energy between the electronic ground and (π, π*) excited states. For the [Ni(tpp)] in the (d, d) excited state, vibrational excitation results mainly from the large electronic energy release upon the nonradiative transition from the (π, π*) excited state to the (d, d) excited state. Upon the nonradiative transition, only accepting or promoting modes are vibrationally excited. Therefore, the electronic delocalization in the porphyrin ring and phenyl groups does not necessarily give rise to the vibrational excitation of the ϕ_4 mode. The present results suggest that the ϕ_4 mode is a poor accepting or promoting mode.

Summary

We have successfully applied picosecond TR^3 spectroscopy to explore the vibrational dynamics of [Ni(tpp)] in the (d, d) excited state. This study elucidated that the transient Stokes Raman scattering originating from the (d, d) excited state appears instantaneously upon the photoexcitation and decays with a time constant of ~250 ps, which is consistent with the results of the ultrafast absorption measurements reported previously.[53] The anti-Stokes kinetics gives some insight into the VER following the nonradiative transition. Three in-plane vibrational modes, ν_1, ν_2, and ν_4, showed anti-Stokes intensity decay of about 3.5 ps. This was ascribed to IET of [Ni(tpp)] in the (d, d) excited state. In the course of the IET, the anti-Stokes ϕ_4 band was not observed at any time delay. This means that the ϕ_4 mode is vibrationally less excited than the in-plane vibrational modes on the formation of the (d, d) excited state, and is left less excited in the process of IET, indicating that vibrational energy redistribution into the phenyl peripherals of [Ni(tpp)] is slower than energy dissipation into the solvent molecules.

This work was supported by Grants-in-Aid to Y. M. (11740339) and to T. K. (13308039) from the Ministry of Education, Science, Sports and Culture.

References

1 T. Elsaesser and W. Kaiser, *Ann. Rev. Phys. Chem.*, **42**, 83 (1991).

2 J. C. Owrutsky, D. Raftery, and R. M. Hochstrasser, *Ann. Rev. Phys. Chem.*, **45**, 519 (1994).

3 A. Seilmeier and W. Kaiser, in "Ultrashort Laser Pulses: Generation and Applications," ed by W. Kaiser, Springer-Verlag, Berlin (1993), Vol. 60, pp. 279.

4 G. W. Robinson and R. P. Frosch, *J. Chem. Phys.*, **37**, 1962 (1962).

5 S. H. Lin, *J. Chem. Phys.*, **44**, 3759 (1966).

6 M. Bixon and J. Jortner, *J. Chem. Phys.*, **48**, 715 (1968).

7 A. Mokhtari, J. Chesnoy, and A. Laubereau, *Chem. Phys. Lett.*, **155**, 593 (1989).

8 F. Laermer, T. Elsaesser, and W. Kaiser, *Chem. Phys. Lett.*, **156**, 381 (1989).

9 R. J. Sension, S. T. Repinec, A. Z. Szarka, and R. M. Hochstrasser, *J. Chem. Phys.*, **98**, 6291 (1993).

10 T. Yamaguchi, Y. Kimura, and N. Hirota, *J. Chem. Phys.*, **113**, 2772 (2000).

11 Y. Mizutani and T. Kitagawa, *Science*, **278**, 443 (1997).

12 T. Nakabayashi, H. Okamoto, and M. Tasumi, *J. Phys. Chem. A*, **102**, 9686 (1998).

13 Y. Mizutani, Y. Uesugi, and T. Kitagawa, *J. Chem. Phys.*, **111**, 8950 (1999).

14 S. Hogiu, W. Werncke, M. Pfeiffer, J. Dreyer, and T. Elsaesser, *J. Chem. Phys.*, **113**, 1587 (2000).

15 H. Okamoto, T. Nakabayashi, and M. Tasumi, *J. Phys. Chem. A*, **101**, 3488 (1997).

16 K. T. Schomacker, O. Bangcharoenpaurpong, and P. M. Champion, *J. Chem. Phys.*, **80**, 4701 (1984).

17 J. Qian, S. L. Schultz, G. R. Bradburn, and J. M. Jean, *J. Phys. Chem.*, **97**, 10638 (1993).

18 J. Qian, S. L. Schultz, and J. M. Jean, *Chem. Phys. Lett.*, **233**, 9 (1995).

19 S. L. Schultz, J. Qian, and J. M. Jean, *J. Phys. Chem. A*, **101**, 1000 (1997).

20 T. Nakabayashi, H. Okamoto, and M. Tasumi, *J. Phys. Chem. A*, **101**, 3494 (1997).

21 T. Nakabayashi, H. Okamoto, and M. Tasumi, *J. Phys. Chem. A*, **101**, 7189 (1997).

22 S. Sato and T. Kitagawa, *Appl. Phys. B*, **59**, 415 (1994).

23 T. Kitagawa, M. Abe, and H. Ogoshi, *J. Chem. Phys.*, **69**, 4516 (1978).

24 M. Abe, T. Kitagawa, and Y. Kyogoku, *J. Chem. Phys.*, **69**, 4526 (1978).

25 X.-Y. Li, R. S. Czernuczewicz, J. R. Kincaid, Y. O. Su, and T. G. Spiro, *J. Phys. Chem.*, **94**, 31 (1990).

26 X.-Y. Li, R. S. Czernuczewicz, J. R. Kincaid, P. Stein, and T. G. Spiro, *J. Phys. Chem.*, **94**, 47 (1990).

27 X.-Y. Li, R. S. Czernuczewicz, J. R. Kincaid, and T. G. Spiro, *J. Am. Chem. Soc.*, **111**, 7012 (1989).

28 J. Rodriguez and D. Holten, *J. Chem. Phys.*, **91**, 3525 (1989).

29 D. Kim, C. Kirmaier, and D. Holten, *Chem. Phys.*, **75**, 305 (1983).

30 Y. Mizutani and T. Kitagawa, *Chem. Rec.*, **1**, 258 (2001).

31 Y. Mizutani, *J. Chem. Phys.*, **109**, 9197 (1998).

32 Y. Uesugi, Y. Mizutani, and T. Kitagawa, *J. Phys. Chem. A*, **102**, 5809 (1998).

33 L. D. Spaulding, C. C. Chang, N.-T. Yu, and R. H. Felton, *J. Am. Chem. Soc.*, **97**, 2517 (1975).

34 T. G. Spiro, J. D. Stong, and P. Stein, *J. Am. Chem. Soc.*, **101**, 2648 (1979).

35 S. Choi, T. G. Spiro, K. C. Langry, K. M. Smith, D. L. Budd, and G. N. La Mar, *J. Am. Chem. Soc.*, **104**, 4345 (1982).

36 W. A. Oertling, A. Salehi, Y. C. Chung, G. E. Leroi, C. K. Chang, and G. T. Babcock, *J. Phys. Chem.*, **91**, 5887 (1987).

37 N. Parthasarathi, C. Hansen, S. Yamaguchi, and T. G. Spiro, *J. Am. Chem. Soc.*, **109**, 3865 (1987).

38 K. Prendendergast and T. G. Spiro, *J. Am. Chem. Soc.*, **114**, 3793 (1992).

39 J. F. Kirner, J. Garofollow, and W. R. Scheidt, *J. Am. Chem. Soc.*, **100**, 6354 (1975).

40 J. L. Hoard, G. H. Cowen, and M. D. Glick, *J. Am. Chem. Soc.*, **89**, 1992 (1967).

41 F. Wondrazek, A. Seilmeier, and W. Kaiser, *Chem. Phys. Lett.*, **104**, 121 (1984).

42 W. Wild, A. Seilmeier, N. H. Gottfried, and W. Kaiser, *Chem. Phys. Lett.*, **119**, 259 (1985).

43 A. M. Weiner and E. P. Ippen, *Chem. Phys. Lett.*, **114**, 456 (1985).

44 A large molecule photoexcited with high energy behaves as if it had a high temperature, although distribution of a total vibrational energy created by photoexcitation is very different from that created by thermal excitation (canonical distribution). Each fundamental mode with frequency $\nu_i < 3000$ cm^{-1} may be considered as a small subsystem of the molecular system of vibrational quantum states. In the case that the energy of the quantum state $h\nu_{\mathrm{i}}$ of the subsystem is small compared to the total energy, the occupation probability of the subsystem is given by $N(\nu_{\mathrm{i}}) = \exp(-h\nu_{\mathrm{i}}/kT)$ in a good approximation. The system, therefore, can be characterized by high "temperature" if the total energy is statistically redistributed over a very large number of isoenergetic states (microcanonical distribution). Kaiser and coworkers called this "internal temperature" [*Chem. Phys. Lett.*, **111**, 326 (1984)].

45 A. P. Shreve and R. A. Mathies, *J. Phys. Chem.*, **99**, 7285 (1995).

46 R. G. Alden, M. C. Schneebeck, M. R. Ondrias, S. H. Courtney, and J. M. Friedman, *J. Raman Spectrosc.*, **23**, 569 (1992).

47 M. C. Schneebeck, L. E. Vigil, and M. R. Ondrias, *Chem. Phys. Lett.*, **215**, 251 (1993).

48 M. C. Simpson, E. S. Peterson, C. F. Shannon, D. D. Eads, J. M. Friedman, C. M. Cheatum, and M. R. Ondrias, *J. Am. Chem. Soc.*, **119**, 5110 (1997).

49 K. Lenz, M. Preiffer, A. Lau, and T. Elsaesser, *Chem. Phys. Lett.*, **229**, 340 (1994).

50 S. S. Eaton and G. R. Eaton, *J. Am. Chem. Soc.*, **97**, 3660 (1975).

51 G. N. LaMar, G. R. Eaton, R. H. Holm, and F. A. Walker, *J. Am. Chem. Soc.*, **95**, 63 (1973).

52 J. M. Burke, J. R. Kincaid, and T. G. Spiro, *J. Am. Chem. Soc.*, **100**, 6077 (1975).

53 H. S. Eom, S. C. Jeoung, D. Kim, J. H. Ha, and Y. R. Kim, *J. Phys. Chem. A*, **101**, 3661 (1997).